Theoretical investigation of the Cs*He$_{n \geqslant 3}$ exciplexes

Mohamed Zbiri *, Claude Daul

Department of Chemistry, University of Fribourg, Chemin du Musée 9, Pérolles, CH-1700 Fribourg, Switzerland

Abstract

The X$^2\Sigma_{1/2}$, A$^2\Pi_{1/2}$, B$^2\Sigma_{1/2}$, and A$^2\Pi_{3/2}$ states of Cs*He$_n$ exciplexes, with $n = \{3, \ldots, 9\}$, are studied using first principle density functional theory (DFT) formalism combined with the zeroth order regular approximation (ZORA). The zero points energies (ZPEs) E_0 for Cs*He$_n$ are calculated at a first step, in order to estimate the stability of the studied exciplexes. Relativistic calculations are carried out including spin–orbit effect (SO), and potential energy surfaces of Cs*He$_6$ are shown. The electronic distribution shapes of the studied molecules are also discussed, and their emission lines are evaluated and compared to a new discovered experimental emission spectra, which has been recently assigned, using a semi-empirical model, to Cs(A$\Pi_{1/2}$)He$_7$. Our first principle calculation suggests that the discovered emission line is most probably due to a decay of Cs(A$\Pi_{1/2}$)He$_6$.

Keywords: Exciplexes; DFT; Electronic density shape; Emission spectra

1. Introduction

Excited atoms often react to form bond electronically excited states of rather unexpected species (alkali-noble-gas combination) which are dissociative in the electronic ground state. Thanks to the extension of the spectral range of the detectors, the discovery of new emission lines is possible. Still one have to characterize and identify the exact molecular states and transitions that are in the origin of the observed radiative process.

The interaction of alkali metals with rare gases has become a fruitful topic of research for both experimentalists and theoreticians, a detailed list of references could be found in Ref. [1]. These complexes serve as model for understanding different kinds of collisional processes such as line broadening, quenching, and electronic energy transfer. This has been assisted significantly by the recent progress in molecular beam technology and cold-atom trapping [2], which has made available many experimental data for these molecules. Alkali-helium exciplexes are formed when

---

* Corresponding author.
  E-mail address: mohamed.zbiri@unifr.ch (M. Zbiri).

one or more He atoms are attracted into the nodal plane of the excited p-orbital of alkali atoms. The formation of Cs*He$_n$ exciplexes have been proposed as the cause of the quenching of fluorescence emission [3,4]. The concept of the chemical bond of exciplexes is crucial, in fact the dispersion forces (van der Waals) is the weakest form of bonding (in the order of 0.1 eV) responsible of the formation of exciplexes, which can be thought of as a dynamically induced dipole interaction between neutral species (for our case Cs and He) that do not have any internal dipole moment. Several empirical and semi-empirical studies attempted to give a clear description of the formation of the exciplexes, and their emission spectra, the two parameters (depth D_e and position R_e) extracted from potential energy surfaces allow to explain the experimental data and to characterize the observed emission lines. The best known model in this field is based on the semi-empirical pair potential model given by Pascale [5]. He used l-dependent pseudopotentials defined from spectroscopical data to describe the e^-–M^+ and e^-–He interactions. Patil [6] made a detailed work, using perturbative expressions, on the adiabatic potentials for alkali-inert gas systems in the ground state. Recently ab initio methods have been used. Kerkines and Mavridis [1,7,8] studied and investigated the $X^2\Sigma^+$, $A^2\Pi$, and $B^2\Sigma^+$ states of LiR exciplexes, where R = {He, Ne, Ar, Kr} using a multi-reference configuration interaction [MRCI] and coupled-cluster plus single and double excitations and a connected triple excitations [CCSD(T)]. Enomoto et al. [9] carried out calculations of adiabatic potential curves of M*He within the restricted Hartree–Fock (RHF) formalism. Kunz [10] performed a configuration interaction (CI) calculations for the Cs–He system based on restricted open shell Hartree–Fock (ROHF) orbitals of Cs obtained from a spin-averaged relativistic calculation using the Douglas–Kroll-transformed spin-free no-pair Hamiltonian (DKH).

Interatomic potentials are of fundamental importance in many physical processes since they determine the sizes of collision cross sections, relaxation and reaction rates as well as the widths and shapes of the spectral lines. Calculation of these potentials are notoriously difficult and experimental verification not easier to obtain. For all the theoretical methods mentioned above, most of them include adjustable model potentials to yield more realistic results. DFT offers the possibility to include dynamical correlations with less computational efforts, we used the relativistic zeroth order regular approximation (ZORA) [11,12] Hamiltonian, which is of zeroth order in the perturbation expansion of $\frac{E}{2mc^2-V}$. The approach is variationally stable and there is no need to renormalization. The spin–orbit operator is regularized and the scalar relativistic corrections are good. There two main gaols of this Letter, the first one is to show that DFT-ZORA approach, which was successfully applied in our previous study [13] for diatomic exciplexes, can describe as well as empirical and semi-empirical methods, exciplex's formation process via reproduction of the potential energy curves for another type of symmetries. The second goal is the investigation of the origin of a new discovered [14] emission line by varying the number of helium atoms n bonded to a Cs atom.

2. Experimental facts

In order to give the reader a complete idea, the experimental observations and assumptions which are in the origin of the discovery of the emission lines of Cs*He$_n$ exciplexes are briefly described here. The existence and formation of alkali-helium exciplexes were considered [14–19] to explain the observed short-time (quenching) atomic fluorescence from excited alkali atoms embedded in different environments such cold helium gas, liquid helium, or in solid helium matrix. Fig. 1 represents energy-level diagram of excited Cs relevant to the observation of Cs atoms, they were excited to the $\mathbf{D_2} : 6S_{1/2} \rightarrow 6P_{3/2}$ and $\mathbf{D_1} : 6S_{1/2} \rightarrow 6P_{1/2}$ transitions. When D_1 excitation is applied, an atomic fluorescence results at the same transition, on other hand, D_2 excitation will produce an emission line from D_1, this is due to the fact that the $6P_{1/2}$ is populated by collisions between Cs atoms in the $6P_{3/2}$ state and helium gas.
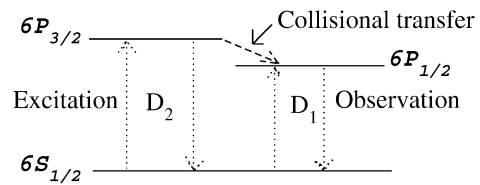

Fig. 1. Energy-level diagram of excited Cs relevant to the observation of Cs atoms.

The fluorescence observed at the transitions D_1 and D_2 depends on the number of the helium atoms that form the molecule, Enomoto et al. [16] conclude that exciplexes with $n > n_{max} = 2$ do not exist, but recently Nettels and coworkers [14] observed and showed that in the hcp phase of solid helium, Cs^*He_n, with $n > 2$ are formed, and for the first time they observe an emission line at 7130 cm^{-1}, which originates from a $Cs^*He_{n \geqslant 3}$ exciplexes.

3. Electronic distribution shape of free excited Cs

The observed emission lines and their quenching are due to the dissociation of the chemical bond formed during the excitation process, the mechanism of the formation of the Cs^*He_n exciplexes could be explained as a consequence of the dynamic behavior of the electronic wave function of excited $Cs(6P_{1/2})$ and $Cs(6P_{3/2})$ when one or more helium atoms approach the excited Cs along a nodal line or around a nodal plane, and overcome the potential barrier, thereby the orbital interaction is more favorite than Pauli repulsion. The shape of the electronic wave function of $6P_{1/2}$ and $6P_{3/2}$ sublevels plays an important role in the explanation of the formation of CsHe$_n$ exciplexes. Below equations of electronic densities and plots of the correspondent electronic wave functions for a free excited Cs are given.

Cs atoms are excited to 6P level which is splitted, due to spin–orbit coupling, into $6P_{1/2}$ and $6P_{3/2}$ sublevels, with total angular momentum $J = L + S$, thus, $M_J = \pm 1/2, \pm 3/2$.

Let us consider an excited Cs atom, the projections are applied on the $|L, M_L, S, M_S\rangle$ basis. We used two normalization constants α and β that verify:

$$|\alpha|^2 + |\beta|^2 = 1.$$

- For $P_{1/2,1/2}$ (i.e., $J = 1/2$ and $|M_J| = 1/2$)

$$\Psi_{1/2,1/2} = \alpha|1, 1, 1/2, -1/2\rangle - \beta|1, 0, 1/2, 1/2\rangle. \quad (1)$$

With $|1, 1, 1/2, -1/2\rangle = |1, 1\rangle \otimes |1/2, -1/2\rangle$, $|1, 0, 1/2, 1/2\rangle = |1, 0\rangle \otimes |1/2, 1/2\rangle$, and $\langle S, M_S | S, M_S'\rangle = \delta_{M_S, M_S'}$, Eq. (1) become

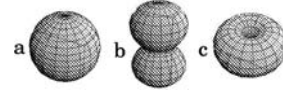$$|\psi_{1/2,1/2}|^2 = |\alpha|^2 \langle 1, 1|1, 1\rangle - |\beta|^2 \langle 1, 0|1, 0\rangle. \quad (2)$$

Fig. 2. Electronic distributions of free Cs in its lowest excited levels: (a) spherical distribution of $6P_{1/2}$ level ($|M_J| = 1/2$), (b) and (c) respectively are dumbbell shaped and apple-like distributions of $6P_{3/2}$ levels ($|M_J| = 1/2, 3/2$).

We can rewrite Eq. (2) in term of spherical harmonics form, with $Y_1^1 = -1/2 \, (3/2\pi)^{1/2} \sin\theta e^{-i\phi}$, $Y_1^0 = 1/2 \, (3/\pi)^{1/2} \cos\theta$.
For $\alpha = (2/3)^{1/2}$ and $\beta = (1/3)^{1/2}$

$$|\psi_{1/2,1/2}|^2 = (1/4\pi)(\cos^2\theta + \sin^2\theta). \quad (3)$$

- For $J = 3/2$, $|M_J| = 1/2, 3/2$
- $P_{3/2,1/2}$

$$\Psi_{3/2,1/2} = (1/3)^{1/2}|1, 1, 1/2, -1/2\rangle$$
$$+ (2/3)^{1/2}|1, 0, 1/2, 1/2\rangle. \quad (4)$$

Using the same arguments as for Eq. (2), Eq. (4) become

$$|\psi_{3/2,1/2}|^2 = (1/2\pi)(\cos^2\theta + (1/4)\sin^2\theta). \quad (5)$$

- $P_{3/2,3/2}$

$$\Psi_{3/2,3/2} = |1, 1, 1/2, 1/2\rangle. \quad (6)$$

Which yields to

$$|\psi_{3/2,3/2}|^2 = (3/8\pi)\sin^2\theta. \quad (7)$$

Fig. 2 shows plots of the electronic wave functions of the excited 6P levels of the free atomic Cs that correspond to Eqs. (3), (5) and (7), we can see the spherical character (Fig. 2(a)) of the density shape of $6P_{1/2}$ ($|M_J| = 1/2$), the dumbbell-shaped and apple-shaped electronic densities (respectively Fig. 2(b) and (c)) of $6P_{3/2}$ ($|M_J| = 1/2, 3/2$). When helium atoms approach the excited Cs, the spherical electronic wave function of $6P_{1/2}$ will change according to the number of helium atoms.

4. Formation process of Cs^*He_n

The formation of the $Cs^*He_{n=1}$ exciplex results when one helium atom approach the excited $Cs(A\Pi_{1/2})$, the spherical electronic wave function

3

Table 1
The corresponding planar symmetries of $Cs^*He_{n>2}$ exciplexes due to their dumbbell shaped electronic distribution

	$CsHe_3$	$CsHe_4$	$CsHe_5$	$CsHe_6$	$CsHe_7$	$CsHe_8$	$CsHe_9$
Symmetry	D_{3h}	D_{4h}	D_{5h}	D_{6h}	D_{7h}	D_{8h}	D_{9h}

(Fig. 2(a)) is deformed and holds an apple-like shape (Fig. 2(c)), this yields to $Cs^*He_{n=1}$ exciplex. A second helium approaches from the opposite side along the nodal line the electronic distribution of the apple-shaped density of Cs–He, which yields to Cs^*He_2 exciplex. We have to note that only the first He has to overcome the energy barrier in order to form the apple-like electronic configuration of a Cs^*He_1 structure. After the formation of the $CsHe_{n=1,2}$, with the two helium atoms bonded along the nodal line of the apple-like density of Cs, now a third helium atom sufficiently close to $Cs(A\Pi_{1/2})$ and after overcoming a potential barrier, will deform the electronic configuration which holds a dumbbell shape (Fig. 2(b)). This new structure has now an attractive potential on further helium atoms located on a ring in the nodal plane (waist) of the dumbbell structure. The repulsion between the helium atoms increases and puts limit on the maximum number $n = n_{max}$. Table 1 represents the corresponding planar symmetries D_{nh} of the $Cs^*He_{n \geqslant 3}$ exciplexes.

5. Computational details

We carried out a relativistic density functional calculations of $X^2\Sigma_{1/2}$, $A^2\Pi_{1/2}$, $B^2\Sigma_{1/2}$, and $A^2\Pi_{3/2}$ states of Cs^*He_n (with $n = \{3, \ldots, 9\}$) exciplexes within the ZORA [11,12] formalism with spin–orbit coupling using the Amsterdam density functional (ADF) package [20,21], version (2004.01). Both the local density approximation (LDA) and the generalized gradient approximation (GGA) for exchange-correlation functionals were used. The LDA was applied with the Vosko, Wilk, and Nusair functional [22]. The GGA was applied by using the Perdew–Wang (PW91) functional [23]. The frozen-core approximation for the inner core-electrons was used. The orbitals up to 4d for cesium (Cs) were kept frozen. The valence shells were described by a high diffuse basis, ZORA triple-ζ STO set plus two polarization functions (ZORA/TZ2P) [24], the choice of this basis set

is based on the role of the polarization of Cs and He atoms. The accuracy of the results is influenced by type of the numerical grid [25], since integrals in ADF are evaluated by numerical quadrature [26]. We found that for relativistic studies of weak interactions very fine and high numerical integration grid is needed.

Zero point energies (ZPEs), E_0, calculations were performed with the Gaussian03 program package [27], using the B3LYP hybrid functional [28]. The LANL2DZ [29–31] basis set was adopted for the Cs atom. For the helium atom, a correlation-consistent basis set cc-pV4Z of Dunning [32] was used.

6. Results and discussion

The configuration of valence shell of Cs is $6s^1$. The lowest excitation promotes a 6s electron to 6p orbital. Most of the spin–orbit effects are due to incomplete shielding by the core electrons whereas most of the chemical forces between atoms are due to the valence electrons, a significant simplification of the problem should be possible in which these two effects are considered separately. This separation has been used [13] by first determining potential curves neglecting the spin–orbit effect in the ZORA Hamiltonian, and then calculating potential curves including this effect. We have studied [13] diatomic exciplexes (M^*He, $M = \{Li, Na, K, Rb, Cs, Fr\}$), and showed the effect of the spin–orbit coupling and the capacity of ZORA-DFT, as first principle method, to yield to results in a good agreement with the experiment and the other ab initio and semi-empirical methods [5,9, 10,33–36].

It was assumed [16] that exciplexes $Cs^*He_{n \geqslant 3}$ do not exist, but recent experiments done by Nettels and coworkers [14] showed the existence of new range of emission lines attributed to $Cs^*He_{n \geqslant 3}$, especially emission line at $7130 \, cm^{-1}$. They used Pascale's semi-empirical model [5,37] to calculate and identify the electronic spectra of $Cs^*He_{n \geqslant 3}$, and they concluded that the emission line at $7130 \, cm^{-1}$ originates from decay of $Cs^*He_{n=7}$. Thus, Nettels and coworkers assumed that $n = 7$ is the most likely number of bond atoms, taking into account that the cases $n = 5$ and $n = 6$ are also probable.
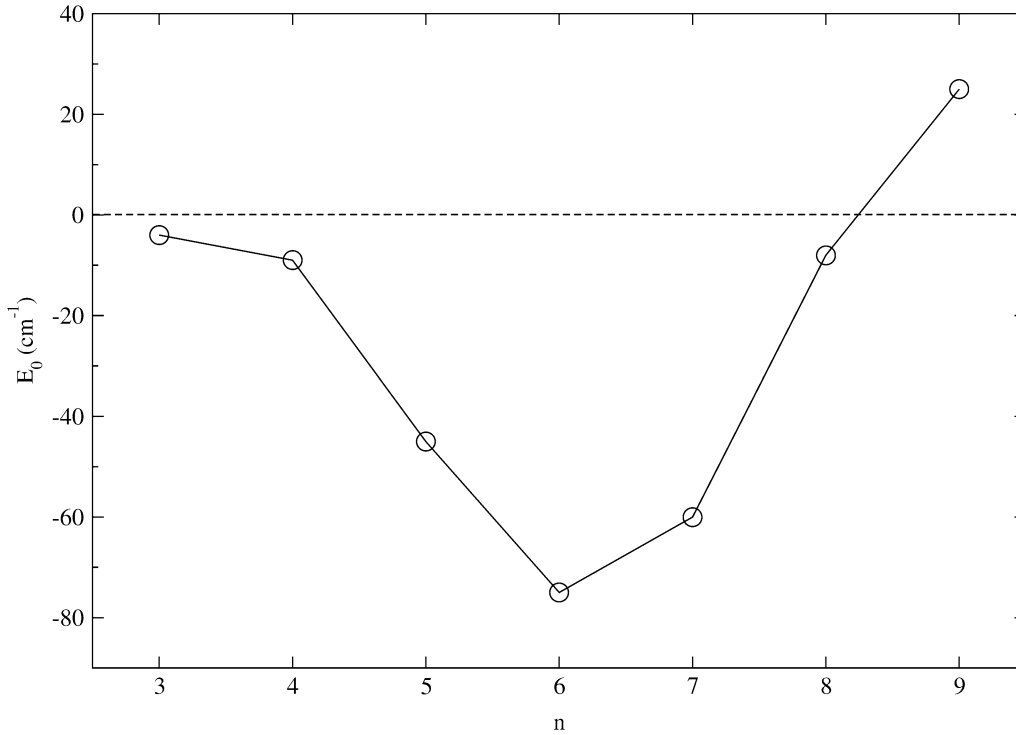
4

Fig. 3. Zero point energies E_0 of the $Cs(A\Pi_{1/2})He_{n \geqslant 3}$ exciplexes as a function of the number n of helium atoms.

Table 2
Calculated emission lines (cm^{-1}) for $Cs(A\Pi_{1/2})He_{n=5,6,7}$ exciplexes, the observed emission line at 7130 cm^{-1} of $Cs(A\Pi_{1/2})He_{n>2}$ is also reported

Calculated			Experiment [14]
$Cs(A\Pi_{1/2})He_5$	$Cs(A\Pi_{1/2})He_6$	$Cs(A\Pi_{1/2})He_7$	$Cs(A\Pi_{1/2})He_{n>2}$
7640	6960	6566	7130

Results presently reported are carried out on Cs^*He_n, with $n = \{3, 4, 5, 6, 7, 8, 9\}$ as described in Section 5. The zero point energies, presented in Fig. 3, are calculated to evaluate the stability of the exciplexes. The $Cs(6^2P_{1/2})He_{n=3,4,8}$ exciplexes have a zero point energies close to the dissociation limit. Due to the strong localization of helium atoms, the $Cs(6^2P_{1/2})He_{n=9}$ exciplex has a zero point energy that is above the dissociation limit. So, the complexes with $n = 3, 4, 8$ and 9, are unstable. It is clearly shown that the $Cs(6^2P_{1/2})He_{n=6}$ exciplex is the most stable one, other possible stable exciplexes are $Cs(6^2P_{1/2})He_{n=5}$ and $Cs(6^2P_{1/2})He_{n=7}$ that have also a zero point energies well below the dissociation limit. Adiabatic potential curves of the $Cs(6^2P_{1/2})He_{n=6}$ complex are

showed in Fig. 4. The lowest potential curve is for the $X^2\Sigma_{1/2}$ state which corresponds to $Cs(6^2S_{1/2}) + 6He$, this potential curve is repulsive. The potential curves with the highest energy among the three excited states are for The $A^2\Pi_{3/2}$ and $B^2\Sigma_{1/2}$ states corresponding to $Cs(6^2P_{3/2}) + 6He$. These potential curves are also repulsive, so they do not exhibit a well to make a bond or a quasi-bond. The $A^2\Pi_{1/2}$ state corresponding to $Cs(6^2P_{1/2}) + 6He$, has a well predicted at about 3.5 Å deep enough to form a bond and can bind more than two helium atoms. This potential has also a barrier at 6 Å which is in very good agreement with the data of Ref. [14]. From the calculated emission lines of $Cs(A\Pi_{1/2})He_{n=5,6,7}$ exciplexes, presented in Table 2, and compared to the observed spectra at
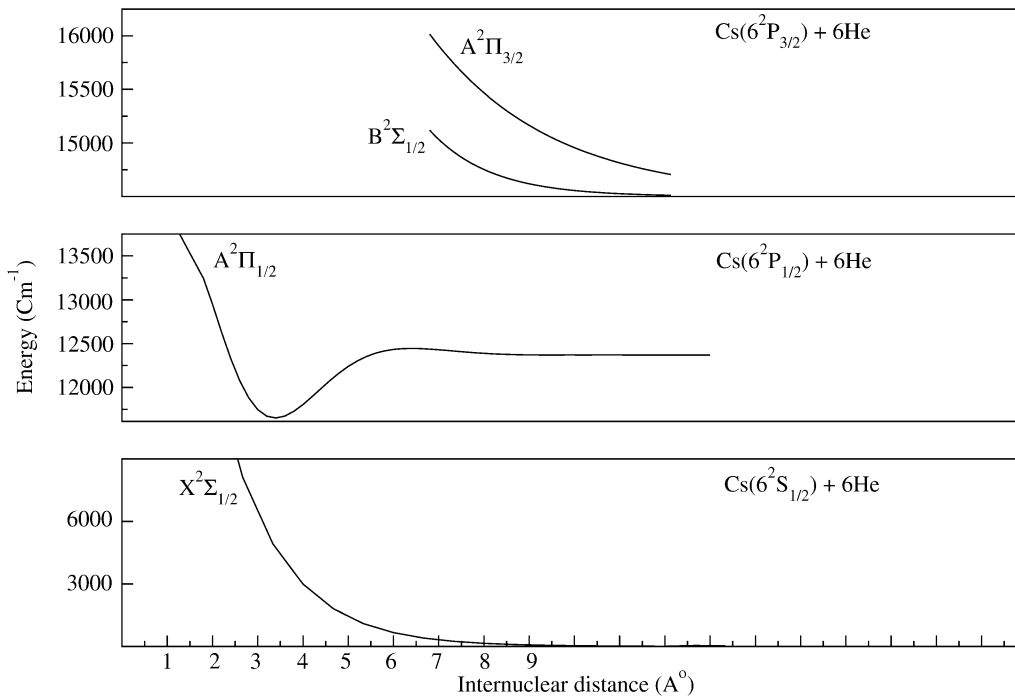
5

Fig. 4. Cs*He$_6$ potential curves. Only the A$^2\Pi_{1/2}$ potential has an attractive well deep enough to make a bond.

Table 3

As a function of the number n ($n \geqslant 3$) of helium atoms, this table represents the radii of the potential minima R_e (in Å), depth of the attractive potential wells D_e (in cm^{-1}), and barrier heights H_b (in cm^{-1}) for the Cs(A$^2\Pi_{1/2}$)He$_n$ exciplexes

n	3	4	5	6	7	8	9
R_e	3.51	3.51	3.50	3.49	3.52	3.53	3.55
D_e	88	285	459	570	581	590	596
H_b	176	172	170	167	164	160	157

7130 cm^{-1}, we can conclude that the most probable origin of the observed emission line is a decay of Cs(A$\Pi_{1/2}$)He$_{n=6}$.

As a function of the number n of helium atoms, data in Table 3 shows:

• The radii of the potential minima, R_e. For $3 \leqslant n \leqslant 6$, the radii decrease with increasing n, and for $6 < n \leqslant 9$, the radius increases rapidly due to the He–He repulsion.

• Depth of the attractive potential wells, D_e. The deepest potential is for the exciplex with $n = 9$, but

this complex is unstable because of its zero point energy that exceeds the dissociation limit.

• The barrier heights, H_b. As shown, the barrier decreases slightly with an increasing number of helium atoms.

7. Summary and concluding remarks

Employing DFT formalism combined with ZORA approach, we have performed relativistic calculations for the X$^2\Sigma_{1/2}$, A$^2\Pi_{1/2}$, B$^2\Sigma_{1/2}$, and A$^2\Pi_{3/2}$ states of Cs*He$_{n \geqslant 3}$ exciplexes. The zero point energies were also evaluated using the B3LYP hybrid functional. In spite of the limitation of DFT to describe and predict high order excited states, it was successfully applied to the ground and lowest excited states of a new type of molecular species, the Cs*He$_n$ exciplexes. The present work concludes that exciplexes with $n \geqslant 3$ can be formed, and their decay can be observed and measured. The observed emission line at 7130 cm^{-1} is therefore originates from a decaying Cs(A$^2\Pi_{1/2}$)He$_{n \geqslant 3}$. Results presently re-

ported show that there are three possible stable exciplexes $Cs(A^2\Pi_{1/2})He_{n=5,6,7}$, but the most likely number of bound helium atoms is $n=6$, this is due to the following facts. (i) The ZPE of that complex is clearly below the dissociation limit. (ii) The calculated emission line, 6960 cm^{-1}, of $Cs(A^2\Pi_{1/2})He_6$ is in very good agreement with the observed spectra at 7130 cm^{-1}. As a final remark, in addition to the first principle methods and calculations presented in this work, semi-empirical results [14] obtained by Nettels and coworkers yield to the same conclusion, the $CsHe_{n\geqslant 3}$ exciplexes exist, and their decay can be observed.

Acknowledgements

References

[1] I.S.K. Kerkines, A. Mavridis, J. Chem. Phys. 116 (21) (2002) 9305.
[2] H.R. Thorsheim, J. Weiner, P.S. Julienne, Phys. Rev. Lett. 58 (1987) 2420.
[3] G. York, R. Scheps, A. Gallagher, J. Chem. Phys. 63 (1975) 1052.
[4] R. Scheps, Ch. Ottinger, G. York, A. Gallagher, J. Chem. Phys. 63 (1975) 2581.
[5] J. Pascale, Phys. Rev. A 28 (1983) 632.
[6] S.H. Patil, J. Chem. Phys. 94 (12) (1991) 8089.
[7] I.S.K. Kerkines, A. Mavridis, J. Phys. Chem. A 104 (2000) 408.
[8] I.S.K. Kerkines, A. Mavridis, J. Phys. Chem. A 105 (2001) 1983.
[9] K. Enomoto, K. Hirano, M. Kumakura, Y. Takahashi, T. Yabuzaki, Phys. Rev. A 69 (2004) 12501.
[10] C.F. Kunz, B.A. Hess, J. Chem. Phys. 112 (2000) 1383.
[11] E. van Lenthe, J.G. Snijders, E.J. Baerends, J. Chem. Phys. 105 (1996) 6505.
[12] E. van Lenthe, R. van Leeuwen, E.J. Baerends, J.G. Snijders, Int. J. Quantum Chem. 57 (1996) 281.
[13] M. Zbiri, C. Daul, J. Chem. Phys. 121 (23) (2004) 11625.
[14] D. Nettels, A. Hofer, P. Moroshkin, R. Muller-Siebert, S. Ulzega, A. Weis, Phys. Rev. Lett. 94 (2005) 63001.
[15] J. Dupont-Roc, Z. Phys. B 98 (1995) 383.
[16] K. Enomoto, K. Hirano, M. Kumakura, Y. Takahashi, T. Yabuzaki, Phys. Rev. A 66 (2002) 42505.
[17] K. Hirano, K. Enomoto, M. Kumakura, Y. Takahashi, T. Yabuzaki, Phys. Rev. A 68 (2003) 12722.
[18] F. Stienkemeier, J. Higgins, C. Callegari, S.I. Kanorsky, W.E. Ernst, G. Scoles, Z. Phys. D 38 (1996) 253.
[19] C. Schulz, P. Claas, F. Stienkemeier, Phys. Rev. Lett. 87 (2001) 153401.
[20] G. te Velde, F.M. Bickelhaupt, E.J. Baerends, C. Fonseca Guerra, S. van Gisbergen, J.G. Snijders, T. Ziegler, J. Comput. Chem. 22 (2001) 931.
[21] C. Guerra, J. Snijders, G. te Velde, E.J. Baerends, Theor. Chem. Accel. 99 (1998) 391.
[22] S.H. Vosko, L. Wilk, M. Nusair, Can. J. Phys. 58 (1980) 1200.
[23] J.P. Perdew, J.A. Chevary, S.H. Vosko, K.A. Jackson, M.R. Pederson, D.J. Singh, C. Fiolhais, Phys. Rev. B 46 (1992) 6671.
[24] E. van Lenthe, E.J. Baerends, J. Comput. Chem. 24 (2003) 1142.
[25] P.M. Boerrigter, G. te Velde, E.J. Baerends, Int. J. Quantum Chem. 33 (1988) 87.
[26] G. te Velde, E.J. Baerends, J. Comput. Phys. 99 (1992) 84.
[27] M.J. Frisch, G.W. Trucks, H.B. Schlegel, G.E. Scuseria, M.A. Robb, J.R. Cheeseman, J.A. Montgomery Jr., T. Vreven, K.N. Kudin, J.C. Burant, J.M. Millam, S.S. Iyengar, J. Tomasi, V. Barone, B. Mennucci, M. Cossi, G. Scalmani, N. Rega, G.A. Petersson, H. Nakatsuji, M. Hada, M. Ehara, K. Toyota, R. Fukuda, J. Hasegawa, M. Ishida, T. Nakajima, Y. Honda, O. Kitao, H. Nakai, M. Klene, X. Li, J. E. Knox, H.P. Hratchian, J.B. Cross, V. Bakken, C. Adamo, J. Jaramillo, R. Gomperts, R.E. Stratmann, O. Yazyev, A.J. Austin, R. Cammi, C. Pomelli, J.W. Ochterski, P.Y. Ayala, K. Morokuma, G.A. Voth, P. Salvador, J.J. Dannenberg, V.G. Zakrzewski, S. Dapprich, A.D. Daniels, M.C. Strain, O. Farkas, D.K. Malick, A.D. Rabuck, K. Raghavachari, J.B. Foresman, J.V. Ortiz, Q. Cui, A.G. Baboul, S. Clifford, J. Cioslowski, B.B. Stefanov, G. Liu, A. Liashenko, P. Piskorz, I. Komaromi, R.L. Martin, D.J. Fox, T. Keith, M.A. Al-Laham, C.Y. Peng, A. Nanayakkara, M. Challacombe, P.M.W. Gill, B. Johnson, W. Chen, M.W. Wong, C. Gonzalez, J.A. Pople, Gaussian 03, Revision C.02, Gaussian, Wallingford, CT, 2004.
[28] A.D. Becke, J. Chem. Phys. 98 (1993) 5648.
[29] P.J. Hay, W.R. Wadt, J. Chem. Phys. 82 (1985) 270.
[30] W.R. Wadt, P.J. Hay, J. Chem. Phys. 82 (1985) 284.
[31] P.J. Hay, W.R. Wadt, J. Chem. Phys. 82 (1985) 299.
[32] T.H. Dunning, J. Chem. Phys. 90 (1989) 1007.
[33] F. Masnou-Seeuws, J. Phys. B 15 (1982) 883.
[34] J. Reho, J. Higgins, K.K. Lehmann, J. Chem. Phys. 113 (2000) 9694.
[35] M.D. Havey, S.E. Frolking, J.J. Wright, Phys. Rev. Lett. 45 (1980) 1783.
[36] N. Geum, G.H. Jeung, Chem. Phys. Lett. 333 (2001) 314.
[37] J. Pascale, J. Vandeplanque, J. Chem. Phys. 60 (1974) 2278.